Environmental Pollution 245 (2019) 771–779

Contents lists available at ScienceDirect

Environmental Pollution

journal homepage: www.elsevier.com/locate/envpol

Sources and dry deposition of carbonaceous aerosols over the coastal East China Sea: Implications for anthropogenic pollutant pathways and deposition☆

Fengwen Wang [a, b, c, *], Ting Feng [c], Zhigang Guo [b], Yuanyuan Li [b], Tian Lin [d], Neil L. Rose [e]

[a] State Key Laboratory of Coal Mine Disaster Dynamics and Control, Chongqing University, Chongqing, 400030, China
[b] Shanghai Key Laboratory of Atmospheric Particle Pollution and Prevention (LAP^3), Department of Environmental Science & Engineering, Fudan University, Shanghai, 200438, China
[c] Department of Environmental Science, College of Resources and Environmental Science, Chongqing University, Chongqing, 400030, China
[d] State Key Laboratory of Environmental Geochemistry, Institute of Geochemistry, Chinese Academy of Sciences, Guiyang, 550002, China
[e] Environmental Change Research Centre, University College London, Gower Street, London, WC1E 6BT, United Kingdom

ARTICLE INFO

Article history:
Received 8 July 2018
Received in revised form
18 November 2018
Accepted 20 November 2018
Available online 25 November 2018

Keywords:
Organic carbon
Elemental carbon
Char and soot
Aerosols
Sources
Dry deposition
East China Sea

ABSTRACT

75 paired TSP and $PM_{2.5}$ samples were collected over four seasons on Huaniao Island (HNI), an island that lies downwind of continental pollutants emitted from mainland China to the East China Sea (ECS). These samples were analyzed for organic carbon (OC) and elemental carbon (EC), with a special focus on char-EC (char) and soot-EC (soot), to understand their sources, and the scale and extent of pollution and dry deposition over the coastal ECS. The results showed that char concentrations in $PM_{2.5}$ and TSP averaged from 0.13 to 1.01 and 0.31–1.44 μg m^{-3}; while for soot, they were from 0.03 to 0.21 and 0.16–0.56 μg m^{-3}, respectively. 69.0% of the char and 36.4% of the soot were present in $PM_{2.5}$. The char showed apparent seasonal variations, with highest concentrations in winter and lowest in summer; while soot displayed maximum concentrations in fall and minimum in summer. The char/soot ratios in $PM_{2.5}$ averaged from 3.29 to 17.22; while for TSP, they were from 1.20 to 7.07. Both of the ratios in $PM_{2.5}$ and TSP were highest in winter and lowest in fall. Comparisons of seasonal variations in OC/EC and char/soot ratios confirmed that char/soot may be a more effective indicator of carbonaceous aerosol source identification than OC/EC. Annual average atmospheric dry deposition fluxes of OC and EC into ECS were estimated to be 229 and 107 μg m^{-2} d^{-1}, respectively, and their deposition fluxes significantly increased during episodes. It was estimated that the loadings of OC + EC and EC accounted for 1.3% and 4.1% of the total organic carbon and EC in ECS surface sediments, respectively, implying a relatively small contribution of OC and EC dry deposition to organic carbon burial. This finding also indicates a possibly more important contribution of wet deposition to organic carbon burial in sediments of ECS, and this factor should be considered for future study.

1. Introduction

Organic carbon (OC) is a mixture of hundreds of organic compounds including *n*-alkanes, aromatic and aliphatic compounds. They are formed by both primary emissions from anthropogenic combustion and secondary organic formation through reactions within atmospheric gases. By contrast, elemental carbon (EC) is a mixture of graphite-like particles and light-absorbing organic matter, produced by the incomplete combustion of fossil-fuels and biomass burning, and from the vapor phase as a condensation product. Compared with OC, EC has received much more attention in recent decades due to its significant fossil-fuel combustion source, its adverse effects on human health (Menon et al., 2002; Highwood and Kinnersley, 2006) as well as its potential contribution to global climate change (Schmidt et al., 2001). EC may be divided into two parts: char and soot. Char includes solid residues formed at combustion temperatures between 300 and 600 °C and with a typical particle size range of 1–100 μm; while soot particles

☆ This paper has been recommended for acceptance by Eddy Y. Zeng.

* Corresponding author. State Key Laboratory of Coal Mine Disaster Dynamics and Control, Chongqing University, Chongqing, 400030, China.
E-mail address: fengwenwang@cqu.edu.cn (F. Wang).

https://doi.org/10.1016/j.envpol.2018.11.059
0269-7491/

are graphite clusters mainly formed via gas-to-particle conversion under combustion temperatures ≥600 °C. These formation conditions and their physicochemical properties, make char and soot distinct, and therefore effective tools in the assessment of EC sources and their associated long-range transport pathways in the atmosphere (Han et al., 2010; Cao et al., 2013; Wang et al., 2015a).

Atmospheric OC and EC concentrations have increased in recent decades. In China, this has been due to rapid industrialization and urbanization, especially in eastern and southern regions (Cao et al., 2003; Feng et al., 2009) and the composition and sources of these pollutants have therefore been a focus for researchers. For example, Feng et al. (2007) analyzed the carbonaceous compositions of $PM_{2.5}$ on Changdao Island, located on a line separating the Bohai Sea from the Yellow Sea in northern China, and apportioned sources of these pollutants using specific biomarkers. Hou et al. (2011) apportioned the sources of OC and EC in $PM_{2.5}$ that were collected from 2006 to 2007 in Shanghai and investigated the carbonaceous pollutant roles associated with haze episodes in different seasons. Kunwar and Kawmaura (2014) presented one-year data sets of carbonaceous aerosols collected in Okinawa Island, Japan, with the aim of providing insight into the long range transport of anthropogenic aerosols from East Asia, while Li et al. (2017) integrated three-years observations of OC and EC (2013–2015) in $PM_{2.5}$ in the Taiwan Strait and estimated their potential contribution to the formation of $PM_{2.5}$. These studies emphasized the spatio-temporal characteristics of the concentration and sources of carbonaceous pollutants, yet have been unable to provide an insight into the high-resolution formation mechanisms and atmospheric deposition of these pollutants on regional scales.

The East China Sea (ECS) is located near a highly-developed region of China, namely, the Yangtze River Delta (YRD). This region has been reported as the source of many anthropogenic pollutants as well as a transport pathway for pollutants moving downstream from mainland China to the ECS (Hsu et al., 2010; Lin et al., 2013). However, regional atmospheric circulation patterns result in the ECS being a "receptor" for pollutants transported both from YRD and other adjacent regions (i.e., central and northern China) driven by the East Asian monsoon (Gao et al., 1997; Nakamura et al., 2005) as demonstrated by several studies on atmospheric deposition of heavy metals in dust and trace elements in ECS (Hsu et al., 2009; Hsu et al., 2010; Zhang et al., 2010). Recently, comprehensive aerosol studies concerning nutrients, heavy metals and carbonaceous species associated with long-range transport have also been undertaken at Huaniao Island (HNI) in the coastal ECS (Zhu et al., 2013; Guo et al., 2014; Wang et al., 2014, 2015a). However, these studies were limited to low resolution data on the source formation mechanism of carbonaceous aerosols, and did not refer to atmospheric dry deposition of these pollutants. In this current study, 75 paired TSP and $PM_{2.5}$ samples were collected on HNI over four seasons between October 2011 and August 2012. These samples were analyzed for organic carbon (OC) and elemental carbon (EC), with a special focus on char-EC (char) and soot-EC (soot), to understand the sources, pollution characteristics and dry deposition of OC and EC to the ECS. This study therefore represents the first high resolution assessment of carbonaceous aerosol sources and estimates of dry deposition fluxes to the East China Sea, as well as determining the influence of continental atmospheric pathways on the OC and EC budgets to this important coastal region.

2. Material and method

2.1. Sampling site and sample collection

The sampling site of Huaniao Island (HNI) (N30.86°, E122.67°), is ~66 km east of Shanghai (Fig. 1). It has a land area of 3.28 km^2 and a population of approximately 2000. HNI lies in the downwind transport path of the continental outflow to the northwest Pacific, where the prevailing winds move from west to east in winter and spring driven by the East Asian monsoon. There is almost no anthropogenic emission of OC and EC on the island itself, making it an ideal location to assess continental pollutant transport in the marine atmosphere. The sampling apparatus was placed on the roof of a 15 m high building. The $PM_{2.5}$ samples were collected on pre-combusted quartz filters (20 × 25 cm^2, 2600QAT, PALL, USA) at a flow rate of 18 $m^3 h^{-1}$ through a $PM_{2.5}$ sampler (Guangzhou Mingye Huanbao Technology Company). The TSP samples were collected concurrently on pre-combusted quartz filters (9 cm in diameter, QM-A, Whatman, UK) at a flow rate of 4.1 $m^3 h^{-1}$ (Beijing Geological Institute). The sampling period was from October 23, 2011 to August 20, 2012.75 paired $PM_{2.5}$ and TSP samples covering four seasons were collected during this period. Each paired sample started at 0900 on the first day and ended at 0830 on the following day. Two parallel operational sample blanks were obtained in each season. In order to directly compare the pollution characteristics of carbonaceous aerosols between Shanghai and the coastal ECS on HNI, we simultaneously collected $PM_{2.5}$ samples at a "supersite" in urban Shanghai. This site is located on the roof of No 4. Teaching building at Handan campus of Fudan University (31.3° N, 121.5° E), ~112 km away from HNI (Wang et al., 2016) (Fig. 1). The sampling periods and sample collection times were consistent with those collected at HNI. Prior to sampling, the quartz filters at both sites were wrapped in aluminum foil and baked at 450 °C for 4 h in a muffle furnace. Before and after sample collection, these filters were placed in a constant temperature (20 ± 1 °C) and humidity (45 ± 5%) chamber for 24 h. The exposed filters were stored in labelled, sealed valve bags prior to sample analysis.

2.2. Sample analysis

Organic carbon and EC in all samples were detected using a Thermal/Optical Carbon Analyzer (Desert Research Institute: DRI, Model, 2001) by IMPROVE thermal/optical reflectance (TOR) (Chow et al., 1993). The targeted eight carbon fractions including four OC fractions (OC1, OC2, OC3, and OC4), three EC fractions (EC1, EC2, and EC3) and a pyrolyzed carbon fraction (OP), were analyzed based on a 0.544 cm^2 punch area that was taken from each sample. These fractions were produced under selected temperature and oxidation conditions. OC1, OC2, OC3, and OC4 were formed in a helium atmosphere under temperatures of 140 °C, 280 °C, 480 °C and 580 °C, respectively. EC1, EC2 and EC3 were formed in a 2% oxygen/98% helium atmosphere under temperatures of 580 °C, 740 °C and 840 °C, respectively. Details of the TOR method for OC and EC analysis has been previously described by Wang et al. (2015a). OP, defined as the amount of carbon, was measured after the oxygen is added until the reflectance achieves its original value. As a result, OC = OC1+OC2+OC3+OC4+OP, while EC = EC1+EC2+EC3 - OP, respectively. According to Han et al. (2007), char = EC1- OP, and soot = EC2+EC3.

2.3. Dry deposition estimation

Atmospheric dry deposition fluxes of OC and EC in aerosols were parameterized using the methodology previously developed for individual organic compounds such as persistent organic pollutants (Jurado et al., 2004; Park et al., 2001). Dry deposition fluxes of aerosol-bound OC and EC (F_{OC} and F_{EC}, μg m-2 d-1, respectively) were estimated as the product of OC and EC concentrations (i.e. C_{OC} and C_{EC}, μg m^{-3}, respectively) and the corresponding dry deposition velocity of the aerosol particle (D_v, cm/s):

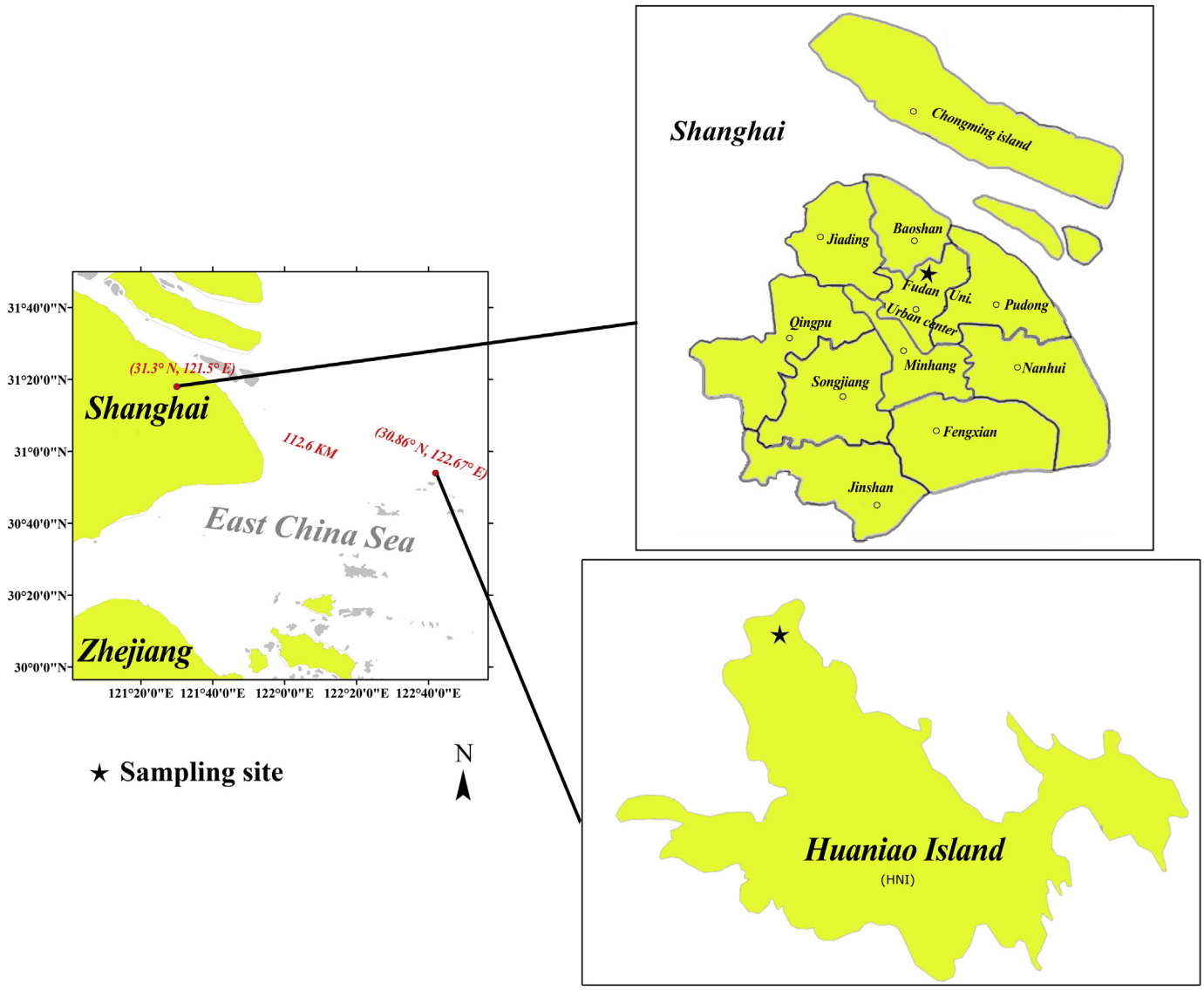

Fig. 1. Map of sampling sites on Huaniao Island (HNI) in coastal ECS and Fudan University in urban Shanghai.

$F_{OC} = D_v \times C_{OC}$

$F_{EC} = D_v \times C_{EC}$

The parameter D_v depends not only on atmospheric turbulence such as wind speed, but also on the aerosol particle size. Previously, a size-segregated sampler (28.3 L min^{-1}, Anderson FA-3) was used to collect aerosol samples for nutrient deposition analysis (Zhu et al., 2013). This sampler collects aerosols into eight stages, namely, 9.0–100 μm (stage 0), 5.8–9 μm (stage 1), 4.7–5.8 μm (stage 2), 3.3–4.7 μm (stage 3), 2.1–3.3 μm (stage 4), 1.1–2.1 μm (stage 5), 0.65–1.1 μm (stage 6), 0.43–0.65 μm (stage 7), and 0–0.43 μm (stage 8). These data were used to provide particle size information for D_v calculations using a particle deposition model. Briefly, D_v is the sum of particle deposition speeds at a series of resistances at the air-surface interface including the aerodynamic resistance and the resistance to molecular diffusion. A detailed description of this methodology is reported elsewhere (Jacobson, 2004). D_v is affected by meteorological conditions including surface temperature and pressure, wind speeds at reference height (10 m), and wind direction. Meteorological data were obtained by a portable Automatic Weather Station (Jinzhou Sunshine Scientific, JW-3) installed at HNI.

2.4. Quality assurance and quality control (QA/QC) procedures

The analyzer was calibrated with sucrose (10.56 μg) every day and the recovery rate was within a difference < 6% for each calibration. Replicate analyses were performed after every ten samples. The difference determined from replicate analyses was 2.9% for OC and EC, 4.1% for TC (total carbon, OC + EC), and 8.3% for char and soot. The blank filters (n = 8) were analyzed using the same procedures as those for the samples. The results presented in this study were calibrated with respect to the concentrations of blank filters.

3. Results and discussion

3.1. Concentrations of char and soot in $PM_{2.5}$ and TSP

Concentrations of char and soot (in μg m^{-3}) and ratios of char/soot and OC/EC in $PM_{2.5}$ and TSP in each season at HNI are shown in

Table 1. The concentrations of char and soot in all $PM_{2.5}$ and TSP samples are shown in Table S1 (supporting information). The average concentrations of char in $PM_{2.5}$ were 0.83 μg m^{-3} in fall, 1.01 μg m^{-3} in winter, 0.85 μg m^{-3} in spring, and 0.13 μg m^{-3} in summer; for TSP, they were 0.94 μg m^{-3}, 1.44 μg m^{-3}, 1.14 μg $m^{-3}$and 0.31 μg m^{-3}, respectively. Soot concentrations, based on a four season average, were 4–8 times lower than the corresponding char. For comparison, Table 1 also summarizes the concentrations of char and soot in $PM_{2.5}$ in Shanghai, collected concurrently with those at HNI. The char and soot were all lower at HNI (0.13–1.01 μg m^{-3} for char, 0.03–0.21 μg m^{-3} for soot) than in Shanghai (1.83–3.75 μg m^{-3} for char, 0.30–0.41 μg m^{-3} for soot), indicating relatively severe carbonaceous pollution and complicated source contributions of these pollutants to the Shanghai atmosphere. 69.0% of the char and 36.4% of the soot were present in the $PM_{2.5}$ fraction at HNI (Table 1). These values are lower than those of the corresponding OC and EC, which were 88% and 80%, respectively (Wang et al., 2015a). The different content of char, soot, OC and EC in $PM_{2.5}$ relative to TSP indicates an important role in source identification of carbonaceous aerosols.

Seasonal variation of char and soot in $PM_{2.5}$ and TSP on HNI is shown in Fig. 2. It can be seen that char shows apparent seasonal variations, with highest concentrations in winter (average: 1.01 μg m^{-3} in $PM_{2.5}$ and 1.44 μg m^{-3} in TSP) and lowest in summer (average: 0.13 μg m^{-3} in $PM_{2.5}$ and 0.31 μg m^{-3} in TSP). Soot displays relatively small seasonal variations, with maximum concentrations in fall (average: 0.21 μg m^{-3} in $PM_{2.5}$ and 0.56 μg m^{-3} in TSP) and minimum concentration in summer (average: 0.03 μg m^{-3} in $PM_{2.5}$ and 0.16 μg m^{-3} in TSP). For a better direct comparison, the individual char and soot concentrations in $PM_{2.5}$ in Shanghai are also presented in Fig. 2 (red dotted line). As shown in Fig. 2, seasonal trends in soot are much less distinct than those of char. The concentrations of soot were similar over four seasons, averaging 0.30 μg m^{-3} in fall, 0.38 μg m^{-3} in winter, 0.41 μg m^{-3}in spring and 0.37 μg m^{-3} in summer, respectively. For char, concentrations are highest in winter (average: 3.75 μg m^{-3}), lowest in summer (average: 1.83 μg m^{-3}), and intermediate in fall and spring, with averages of 3.59 and 2.31 μg m^{-3}, respectively. The different seasonal patterns between HNI and Shanghai indicate that the soot in $PM_{2.5}$ at the two sites may be from different sources.

Table 2 shows a comparison between the mean concentrations of char and soot (μg m^{-3}) in $PM_{2.5}$ at HNI with other studies including background and urban sites worldwide. The char and soot concentrations of $PM_{2.5}$ at HNI (0.71 and 0.12 μg m^{-3}, respectively) were comparable to a remote sampling site at Qinghai Lake, on the Tibetan Plateau (0.32 and 0.12 μg m^{-3}, respectively) (Zhu et al., 2014), but lower than in a village in Wusumu, Inner Mongolia (1.15 and 0.69 μg m^{-3}, respectively) (Han et al., 2008) and a suburban site at Qiongzhou University in Sanya on Hainan Island

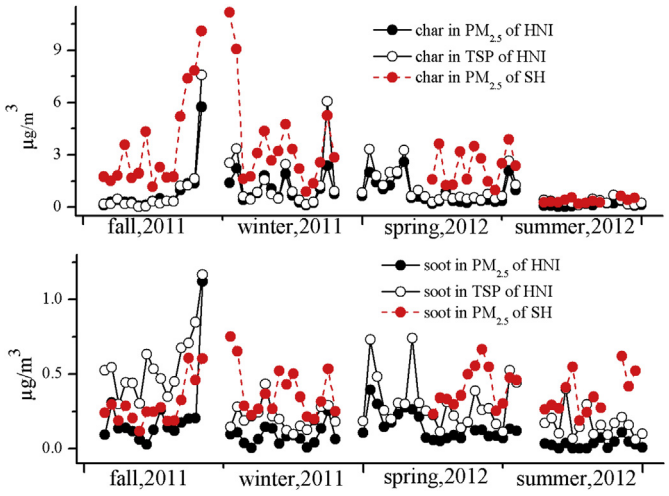

Fig. 2. Seasonal variations of char and soot in $PM_{2.5}$ and TSP (both in μg m^{-3}) on HNI. (Red dotted lines are the individual char and soot concentrations in $PM_{2.5}$ of Shanghai samples that were simultaneously collected). (For interpretation of the references to colour in this figure legend, the reader is referred to the Web version of this article.)

(1.04 and 0.18 μg m^{-3}, respectively) (Wang et al., 2015b) and an urban site at East China University of Science and Technology in Shanghai (1.64 and 0.31 μg m^{-3}, respectively) (Zhao et al., 2015). Compared with other cities, such as Taibei (18.1 and 0.8 μg m^{-3}, respectively) (Zhu et al., 2010) and Xi'an (7.45 and 1.82 μg m^{-3} in urban and 4.1 and 0.5 μg m^{-3} in rural locations, respectively) (Han et al., 2016; Zhu et al., 2016), the concentrations of char and soot at HNI were 5- to 10-fold lower. Comparing these results with those from cities overseas, char concentrations at HNI were lower than those at Bangi in Selangor, Malaysia (Fujii et al., 2016), Saitama in Japan (Kim et al., 2011), Raipur in Chhattisgarh, India (Sahu et al., 2018) and Sonla in Vietnam (Lee et al., 2016), which were 3.85, 2.68, 7.9 and 3.0 μg m^{-3}, respectively. However, soot concentrations were comparable (0.27, 0.30 and 0.4 μg m^{-3} in Malaysia, Japan and Vietnam, respectively), with the exception of where concentrations reached 2.2 μg m^{-3}.

3.2. Source identification from char/soot ratios and comparison with OC/EC

Since the OC/EC ratio at HNI has been used to apportion sources of carbonaceous aerosols in a previous study (Wang et al., 2015a,b), here we focus on source categories implied by char/soot ratios. Char/soot ratios, while similar to ratios of OC to EC, also vary distinctly between different emission sources. As early as

Table 1
Average concentrations of char, soot (μg m^{-3}) and ratios of char/soot, OC/EC in $PM_{2.5}$ and TSP in each season. (TSP samples were not collected in Shanghai and therefore"-"indicate values where these parameters not obtained).

Site	Season	Char			Soot			Char/Soot		OC/EC (Wang et al., 2015a)	
		$PM_{2.5}$	TSP	%	$PM_{2.5}$	TSP	%	$PM_{2.5}$	TSP	$PM_{2.5}$	TSP
HNI	fall	0.83	0.94	88.7	0.21	0.56	38.4	3.29	1.20	3.5	2.8
	winter	1.01	1.44	70.0	0.09	0.21	40.7	17.22	7.07	4.0	4.2
	spring	0.85	1.14	74.4	0.15	0.31	48.2	5.82	3.91	2.8	2.8
	summer	0.13	0.31	42.9	0.03	0.16	18.4	5.51	2.27	6.1	4.2
SH	fall	3.59	–	–	0.30	–	–	11.35	–	2.8	–
	winter	3.75	–	–	0.38	–	–	9.14	–	2.9	–
	spring	2.31	–	–	0.41	–	–	5.87	–	2.7	–
	summer	1.83	–	–	0.37	–	–	4.39	–	3.1	–

Table 2
Comparisons of the mean concentrations of char and soot (μg m^{-3}) in $PM_{2.5}$ and associated indices at HNI in coastal ECS with worldwide studies.

Location	Type of site	Char	Soot	Char/Soot	OC/EC	Reference
Coastal East China Sea	remote island	0.71	0.12	7.96	5.19	This study
Qinghai Lake	remote area	0.32	0.12	4.3	2.3	Zhu et al. (2014)
Wusumu, Inner Mongolia	remote mountains	1.15	0.69	1.8	6.4	Han et al. (2008)
Sanya	suburban	1.04	0.18	7.59	2.87	Wang et al. (2015b)
Shanghai	urban	1.64	0.31	6.50	5.43	Zhao et al. (2015)
Taibei	urban tunnel	18.1	0.8	20.0	1.26	Zhu et al. (2010)
Xi'an	urban	7.45	1.82	4.55	2.04	Han et al. (2016)
Huxian County, Xi'an	rural	4.1	0.5	8.9	18.1	Zhu et al. (2016)
Bangi, Selangor, Malaysia	urban	3.85	0.27	14.53	2.69	Fujii et al. (2016)
Saitama, Japan	urban	2.68	0.30	13.23	1.91	Kim et al. (2011)
Raipur,Chhattisgarh, India	urban	7.9	2.2	3.56	3.52	Sahu et al. (2018)
Sonla, Vietnam	urban	3.0	0.4	9.6	6.8	Lee et al. (2016)

1999–2000, Chow et al. (2004) found char/soot ratios of 0.60 for motor vehicle exhaust, 1.31 for coal combustion and 22.6 for biomass burning. This ratio was further investigated by Cao et al. in a sampling campaign in Xi'an, China, during the fall and winter of 2003, where ratios of 1.9 where identified for coal combustion and 11.6 for biomass burning. Recently, Han et al. (2010), also conducting a sampling campaign in Xi'an, found char/soot ratio of >3 for biomass burning and coal combustion samples, and <1.0 for motor vehicle exhausts. Therefore, the lower char/soot ratios from vehicular exhaust when compared with biomass burning and coal combustion, may be used for source apportionment of carbonaceous aerosols.

Table 1 summarizes the averaged char/soot and OC/EC ratios for both $PM_{2.5}$ and TSP over the four seasons. Char/soot ratios display pronounced seasonal trends, being highest in winter (17.22 and 7.07 in $PM_{2.5}$ and TSP, respectively) and lowest in fall (3.29 and 1.20 in $PM_{2.5}$ and TSP, respectively). By contrast, seasonal variations in the ratios of OC/EC, are relatively narrow, ranging from 2.8 to 6.1 in $PM_{2.5}$ and 2.8 to 4.2 in TSP, respectively. The higher char/soot ratio in winter suggests a dominance of biomass burning and coal combustion; while lower char/soot in fall and summer indicates the major influence of vehicular exhausts. However, unlike char/soot, OC/EC ratios showed two peaks in winter and summer. The peak in winter could be associated with air parcels transported from northern China (Wang et al., 2015a) where coal combustion is commonly used for indoor heating in winter. The peak in summer could be explained by the formation of secondary organic carbon (SOC) (Feng et al., 2009; Hou et al., 2011) and the influence of shipping traffic including public ferries and cargo transport around Shanghai (Wang et al., 2014, 2017). This suggests that, compared with char/soot, OC/EC is not such a useful parameter in identifying primary sources of carbonaceous aerosols, as it is not only influenced by fuel-type, (i.e. primary emissions), but also by secondary organic aerosol (SOA).

3.3. Correlations between char and soot in $PM_{2.5}$ and TSP

The correlations between char and soot in $PM_{2.5}$ and TSP are plotted in Fig. 3 and Fig. 4 respectively. In $PM_{2.5}$, moderate correlations can be observed between char and soot in winter ($R^2 = 0.61$), spring ($R^2 = 0.46$) and summer ($R^2 = 0.60$), while, in fall, the correlations are lower ($R^2 = 0.22$). For TSP, moderate correlations were also observed in fall and winter ($R^2 = 0.54$ and 0.76, respectively), but were poor in summer ($R^2 = 0.03$). This correlation pattern is similar to those investigated at Lake Daihai, a rural high-mountain area in Inner Mongolia, northern China (Han et al., 2008) and could be due to smaller soot particles being transported over longer distances by prevailing winds; while larger char particles tend to remain closer to emission sources (Masiello, 2004). As for the variation in slope of $PM_{2.5}$ and TSP over the four seasons, this may be explained by increasing contributions of soot to EC in cold seasons (fall and winter) compared to those in spring and summer. This is possibly due to a reduced contribution from biomass burning and coal combustion in warmer seasons.

The correlation indices (R^2) between OC, EC, char, soot, and char/soot, in $PM_{2.5}$ and TSP, are summarized in Table S2. The correlations between char and soot are much weaker than those between OC and EC, indicating contributions from different emission sources for char and soot. Char, both in $PM_{2.5}$ and TSP, showed stronger correlations with OC and EC with respect to soot. This may be explained by the production of char as a residue of incomplete combustion while soot is formed by the transformation of gas to particulate form by condensation. Furthermore, correlations between EC and char ($R^2 = 0.98$ and 0.96 in $PM_{2.5}$ and TSP, respectively) were much stronger than those between EC and soot ($R^2 = 0.37$ and 0.12 in $PM_{2.5}$ and TSP, respectively), indicating the dominant role of char in total EC. This also indicates that EC measured by TOR may be used to estimate char concentrations, which is consistent with previous investigations from both urban and remote rural sites (Han et al., 2007, 2008).

3.4. Dry deposition of OC and EC

Previous estimates of dry deposition fluxes for aerosols have usually been based on TSP concentrations multiplied by TSP dry deposition velocities (Duce et al., 1991; Franz et al., 1998; Gigliotti et al., 2005). However, our previous study showed that 88% OC and 80% EC were found in $PM_{2.5}$ (Wang et al., 2015a), which would suggest an overestimation if we used TSP dry deposition velocities to estimate the flux. Therefore, we used the average deposition velocity (D_v) for particles collected on stages 4–7 (0.43–3.3 μm) and stages 0–3 (3.3–100 μm) to estimate flux for $PM_{2.5}$ and TSP-$PM_{2.5}$, respectively. The equations can be described as:

$$D_v\ (PM_{2.5}) = \sum MC_i \times D_{vi} / \sum MC_i\ (i = 4\text{–}7)$$

$$D_v\ (\text{TSP-}PM_{2.5}) = \sum MC_i \times D_{vi} / \sum MC_i\ (i = 0\text{–}3)$$

where MC_i is the mass concentration of stage i (μg m^{-3}), and D_{vi} is the deposition velocity of stage i (cm s^{-1}).

The average deposition velocity (D_v) and corresponding flux of OC and EC in $PM_{2.5}$ and TSP-$PM_{2.5}$ over the four seasons at HNI are presented in Table S3. $PM_{2.5}$ deposition velocities showed no apparent seasonal differences and averaged 2.43×10^{-2} cm s^{-1}. For TSP-$PM_{2.5}$, deposition velocities were smaller in spring and winter than in fall and summer and averaged 0.46 cm s^{-1}. For $PM_{2.5}$, OC

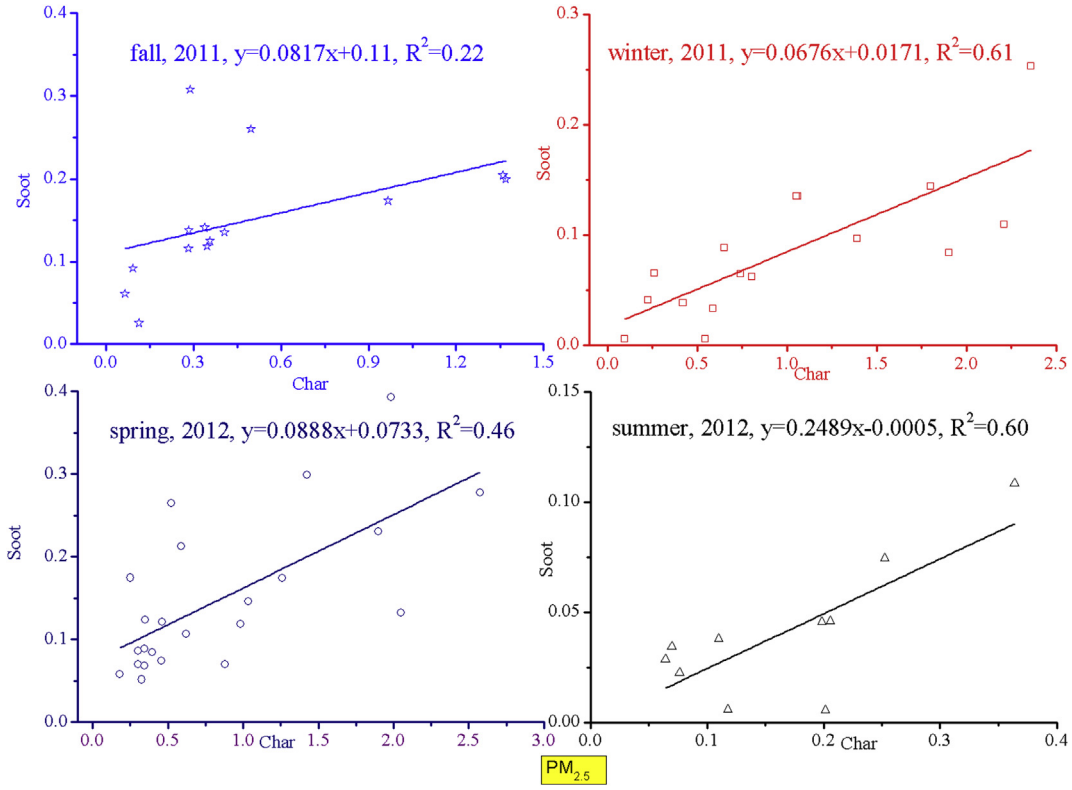

Fig. 3. The correlations between char and soot in $PM_{2.5}$ over four seasons.

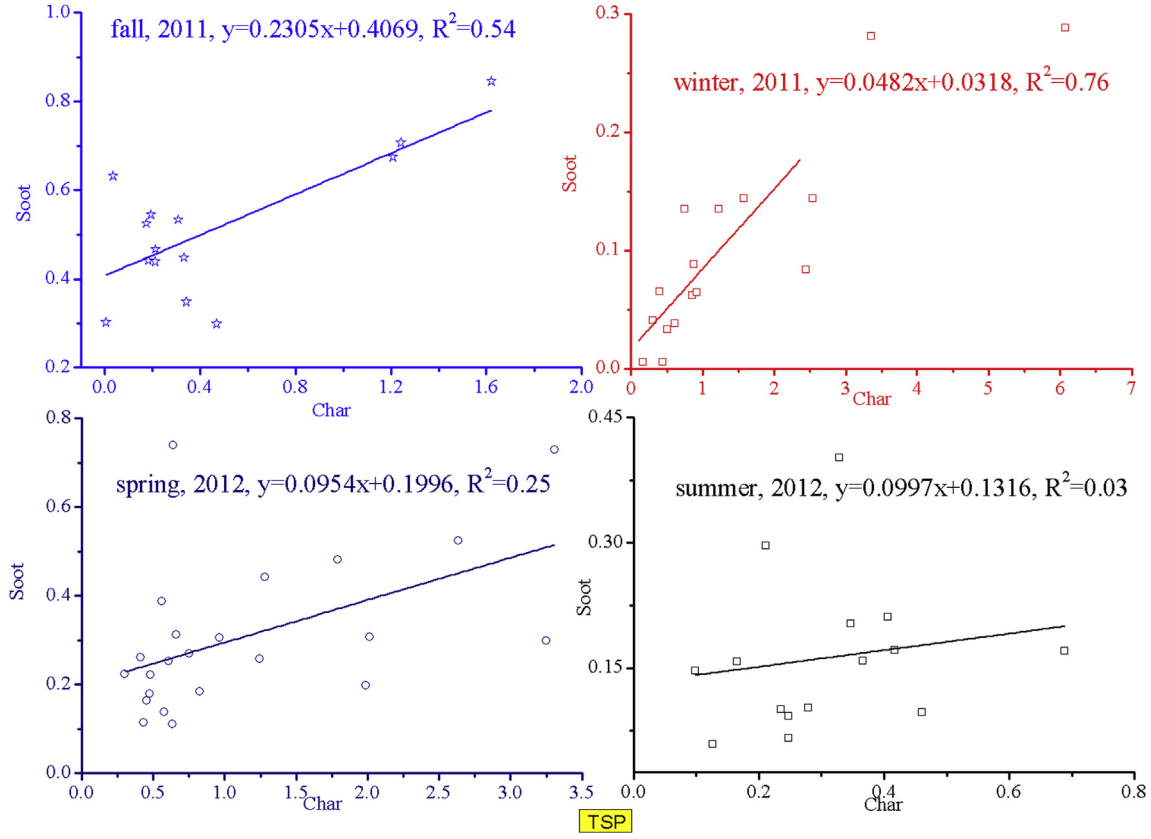

Fig. 4. The correlations between char and soot in TSP over four seasons.

fluxes ranged from 11.4 to 610.8 μg m^{-2} d^{-1} in fall, 19.1–173.7 μg m^{-2} d^{-1} in winter, 18.8–235 μg m^{-2} d^{-1} in spring and 8.5–63.4 μg m^{-2} d^{-1} in summer, with averages of 70.2 μg m^{-2} d^{-1}, 75.1 μg m^{-2} d^{-1}, 67.6 μg m^{-2} d^{-1} and 28.5 μg m^{-2} d^{-1}, respectively. EC fluxes were two-to five-fold lower than the corresponding OC flux. For TSP-$PM_{2.5}$, the OC fluxes were comparable, or two-to three-fold higher, than those in $PM_{2.5}$. The EC flux for TSP-$PM_{2.5}$ comprised most of the total dry deposition flux: about 80% of the annual average. These values are comparable to previously published results. For example, Jurado et al. (2008) reported dry deposition fluxes of 20–210 μg m^{-2} d^{-1} for OC, and 10–30 μg m^{-2} d^{-1} for EC based on measurements taken during an ocean cruise. However, in sub-tropical north-east Atlantic, OC deposition fluxes (11760 ± 2640 μg m^{-2} d^{-1}) were found to be much higher than those observed in this current study (Duarte et al., 2006). These differences suggest spatial variations between regions and uncertainties associated with the dry deposition fluxes using the parameters described above.

In order to understand the relative importance of atmospheric dry deposition to the carbon budget of coastal ECS, we assessed the contribution of OC and EC dry deposition to the ECS OC and EC budgets. Deng et al. (2006) estimated that about 7.4×10^6 t $year^{-1}$ of TOC (OC + EC) were preserved in shelf sediments of the ECS. According to a study on EC preservation in these sediments (Wang and Li, 2007), we used an average of 10% (5%–15% in 3 sampling sites) of EC to TOC to estimate EC burial. This indicates about 7.4×10^5 t $year^{-1}$ of EC preserved in ECS sediments. However, based on the estimate of OC + EC flux in each season and the 7.7×10^5 km^2 area of ECS, an estimated 6.4×10^4 t $year^{-1}$ OC and 3×10^4 t $year^{-1}$ EC would be deposited to ECS. The dry deposition flux of OC + EC would therefore account for 1.3% of the TOC burial while the EC deposition flux would contribute 4.1% of the EC burial in ECS.

Although our study was limited to data collected on an island and did not account for the spatial variation of OC and EC over the ECS, these data sets provide a first insight and estimate of the contribution of dry deposition to total carbon burial in the ECS. Larger scale investigations using cascade impactors at multiple sites are needed to improve this dry deposition estimate. Importantly, there have been several studies on the wet deposition of OC and EC (Cooke and Wilson, 1996; Duce et al., 1991; Jurado et al., 2005). Since wet deposition scavenges particle compounds effectively, wet deposition fluxes of OC and EC should be higher. Jurado et al. (2008) estimated that there were about 47 Tg $year^{-1}$ of OC and 10 Tg $year^{-1}$ of EC in wet deposition to the global ocean and only 11 and 2 Tg $year^{-1}$ in dry deposition. Our study also suggests a vital role for wet deposition on the TOC budget of ECS. Further estimates of the contribution of wet deposition to organic carbon burial in sediments of the coastal ECS would prove to be interesting and fruitful.

3.5. Sources of char and soot and flux of OC and EC during episodes

Three episodes with high concentrations of both char and soot were observed in fall (November 11–13 2011), winter (December 24–25 2011) and spring (March 31-April 1, 2012) (Fig. 2). The air mass pathways during these episodes have been presented in our previous studies (Wang et al., 2014, 2015a) but are included as Fig. S1 in supporting information. In this study, we focus on source identification based on the concentrations and ratios of char and soot and the fluxes of OC and EC in these episodes.

Fig. 5 shows a comparison between average concentrations of char and soot for $PM_{2.5}$ (μg m^{-3}) and dry deposition fluxes of OC and EC for $PM_{2.5}$ and TSP-$PM_{2.5}$ (μg m^{-2} d^{-1}) between normal and episode days. The average concentration of char in $PM_{2.5}$ was 2.82 μg m^{-3} and 0.34 μg m^{-3} in the fall episode days and non-episode days, respectively, a more than eight-fold increase. For soot, these averages were 0.51 μg m^{-3} and 0.14 μg m^{-3}, respectively. Furthermore, the char/soot ratio in the episode was 5.5, while on non-episode days it was 2.4 indicating an increased contribution from biomass burning during the episode (Han et al., 2010). As expected, the deposition fluxes of OC and EC correspondingly increased, 441.5 μg m^{-2} d^{-1} and 73.2 μg m^{-2} d^{-1} for OC, 151.5 μg m^{-2} d^{-1} and 26.1 μg m^{-2} d^{-1} for EC, in the fall episode and non-episode days, respectively. This indicates that biomass burning associated with anthropogenic activity could not only lead to an intensive increase in char and soot concentrations, but could also influence the carbonaceous aerosol budget to the coastal ECS.

The winter episode was not as severe as that in the fall. The concentrations of char were 1.8 μg m^{-3} and 0.9 μg m^{-3} in the episode and non-episode periods, respectively, while for soot, they averaged 0.1 and 0.08 μg m^{-3}, remaining relatively constant before and after the episode. The char/soot ratios in the episode (18.0) were higher than those on non-episode days (11.3). However, the increased rate of deposition of OC and EC were more obvious, 269.8 μg m^{-2} d^{-1} and 151.7 μg m^{-2} d^{-1} for OC, and 109.3 μg m^{-2} d^{-1} and 37.6 μg m^{-2} d^{-1} for EC in the winter episode and non-episode, respectively. According to back-trajectories, the air mass during the episode could be traced back to northern China (Wang et al., 2015a,b). In this region, coal and biomass burning were commonly used for indoor heating in winter. Therefore, we conclude that a possible increase in char and soot trigged by biomass burning and an additional source, such as coal burning, is responsible for the other carbonaceous aerosol components.

The extent of the episode in spring was similar to that of winter. As shown in Fig. 5, the concentrations of char and soot, and the fluxes of OC and EC in the episode (1.7 μg m^{-3}, 0.25 μg m^{-3}, 331.2 μg m^{-2} d^{-1}, 108.4 μg m^{-2} d^{-1}, respectively) were approximately double that of the non-episode (0.55 μg m^{-3}, 0.11 μg m^{-3}, 149.1 μg m^{-2} d^{-1}, 49.6 μg m^{-2} d^{-1}, respectively). The char/soot ratio remained fairly constant thereafter, 6.8 in the episode and 5.0 in the non-episode, respectively. This ratio also exactly characterizes a biomass burning source. According to Wang et al. (2015a), the air mass that arrived at HNI during this spring episode was from northern China, where Asian dust storm events frequently occur, and passed over highly populated eastern China. The dusts from these source areas could be entrained into the free troposphere and subsequently transported to remote areas by prevailing westerly winds (Zhang et al., 1997). Therefore, the spring episode could be attributed to the long-range transport of dusts and pollutants from biomass burning.

4. Conclusions

This study provides the first data sets of atmospheric char and soot, and dry deposition of OC and EC over coastal ECS. The annual average concentrations of char and soot in $PM_{2.5}$ were 0.71 and 0.12 μg m^{-3}, respectively. In TSP, they were 0.96 and 0.31 μg m^{-3}, respectively. The higher char/soot ratio in winter suggests a dominance from biomass burning and coal combustion; while lower char/soot ratios in fall and summer indicate the influence of vehicular exhausts. The stronger correlations between EC and char compared with EC and soot indicate a dominant role of char in total EC. The atmospheric dry deposition fluxes of OC and EC showed a minimum in summer and maximum in winter. It was estimated that the contribution of atmospheric dry deposition fluxes of OC + EC and EC to TOC and EC burial in the ECS were 1.3% and 4.1%, respectively. Three episodes of high char and soot concentrations, as well as deposition fluxes of OC and EC, demonstrated the impacts of anthropogenic pollutant pathways on the sources, pollution

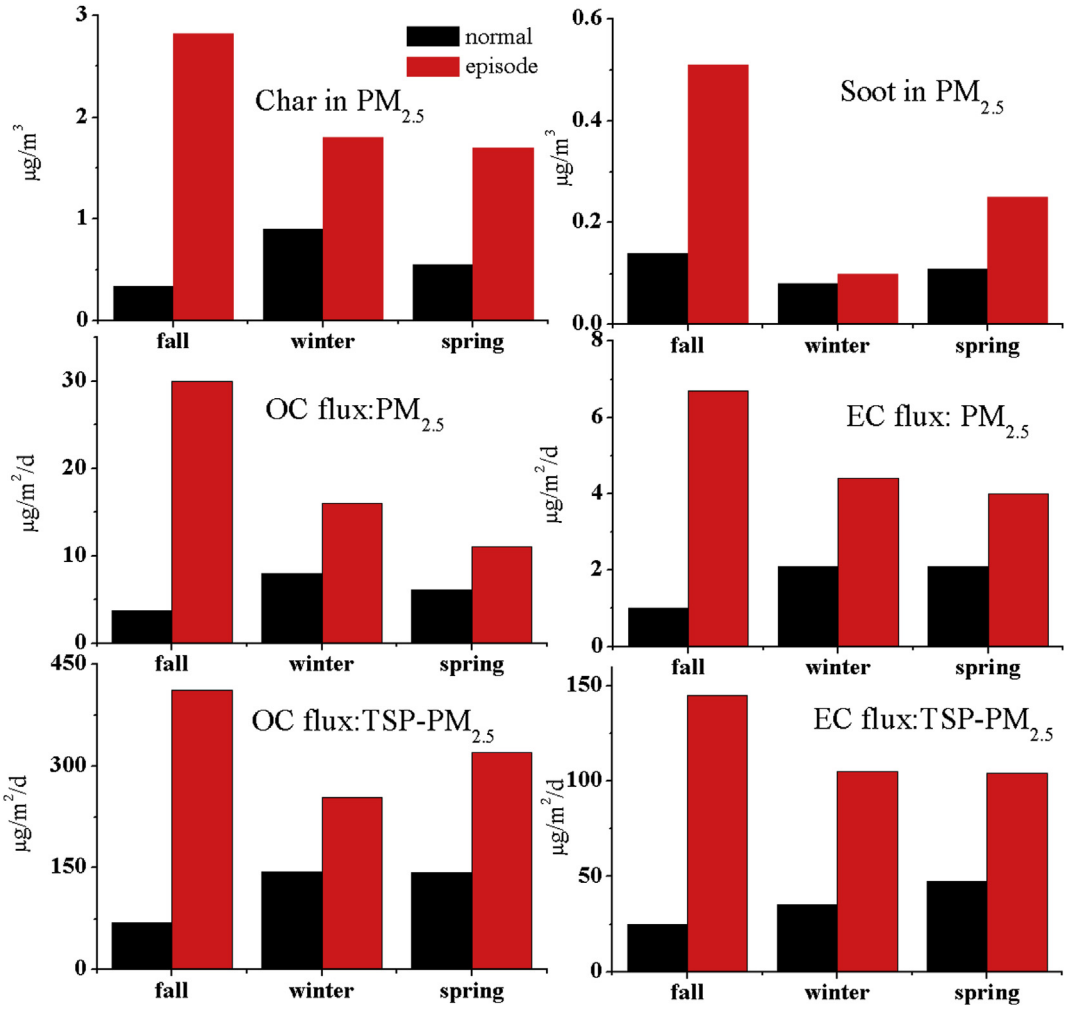

Fig. 5. Comparisons between average concentrations of char and soot for $PM_{2.5}$ (μg m^{-3}) and dry deposition fluxes of OC and EC for $PM_{2.5}$ and TSP-$PM_{2.5}$ (μg m^{-2} d^{-1}) between normal and episodic days.

characteristics and dry deposition of carbonaceous aerosols over the coastal ECS.

Acknowledgements

This work was funded by the National Key R&D Program of China (No: 2018YFC0214000), National Natural Science Foundation of China (NSFC) (No: 41603102), the Opening Project of Shanghai Key Laboratory of Atmospheric Particle Pollution and Prevention (LAP^3) (No: FDLAP16007); and supported by the Fundamental Research Funds for the Central Universities (No: 106112017CDJXY240001). Sincere thanks are given to Mr. Chuanliang Ma and Miss Huaiyu Fu for their great help at sample collection. We also gratefully acknowledge the constructive comments from the anonymous reviewers that greatly improved this work.

Appendix A. Supplementary data

Supplementary data to this article can be found online at https://doi.org/10.1016/j.envpol.2018.11.059.

References

Cao, J.J., Lee, S.C., Ho, K., Zou, S., Zhang, X., Pan, J., 2003. Spatial and seasonal distributions of atmospheric carbonaceous aerosols in Pearl River Delta Region, China. China Particuol. 1, 33–37.

Cao, J.J., Zhu, C.S., Tie, X.X., Geng, H.H., Xu, H.M., Ho, S.S.H., Wang, G.H., Han, Y.M., Ho, K.F., 2013. Characteristics and sources of carbonaceous aerosols from Shanghai, China. Atmos. Chem. Phys. 13 (2), 803–817.

Chow, J.C., Watson, J., Pritchett, L., Pierson, W., Frazier, C., Purcell, R., 1993. The DRI thermal/optical reflectance carbon analysis system: description, evaluation and applications in US air quality studies. Atmos. Environ. 27, 1185–1201.

Chow, J.C., Watson, J.G., Kuhns, H.D., Etyemezian, V., Lowenthal, D.H., Crow, D.J., Kohl, S.D., Engelbrecht, J.P., Green, M.C., 2004. Source profiles for industrial, mobile, and area sources in the Big Bend regional aerosol visibility and observational (BRAVO) study. Chemosphere 54, 185–208.

Cooke, W.F., Wilson, J.J., 1996. A global black carbon aerosol model. J. Geophys. Res. 101, 19395–19409.

Deng, B., Zhang, J., Wu, Y., 2006. Recent sediment accumulation and carbon burial in the East China Sea. Global Biogeochem GB3014. https://doi.org/10.1029/2005GB002559. Cycles 20.

Duarte, C., Dachs, J., Llabrés, M., Alonso-Laita, P., Gasol, J., Tovar-Sánchez, A., Sanñudo-Wilhemy, S., Agustí, S., 2006. Aerosol inputs enhance new production in the subtropical northeast Atlantic. J. Geophys. Res. 111, G04006. https://doi.org/10.1029/2005JG000140.

Duce, R., Liss, P., Merrill, J., Atlas, E., Menard, P., Hicks, P., Miller, J., Prospero, J., Ariomoto, R., Church, T., Ellis, W., Galloway, J., Hansen, L., Jickells, T., Knap, A., Reinhardt, K., Schneider, B., Soudine, B., Tokos, J., Tsunogai, S., Wollast, R., Zhou, M., 1991. The atmospheric input of trace species to the world ocean. Global Biogeochem. Cycles 5, 193–259.

Feng, J.L., Guo, Z.G., Chan, C.K., Fang, M., 2007. Properties of organic matter in $PM_{2.5}$

at Changdao Island, China. A rural site in the transport path of the Asian continental outflow. Atmos. Environ. 41, 1924–1935.
Feng, Y.L., Chen, Y.J., Guo, H.Z., Li, J., Sheng, G.Y., Fu, J.M., 2009. Characteristics of organic and elemental carbon in $PM_{2.5}$ samples in Shanghai, China. Atmos. Res. 92, 434–442.
Franz, T.P., Eisenreich, S.J., Holsen, T.M., 1998. Dry deposition of particulate polychlorinated biphenyls and polycyclic aromatic hydrocarbons to Lake Michigan. Environ. Sci. Technol. 32, 3681–3688.
Fujii, Y., Mahmud, M., Tohno, S., Okuda, T., Mizohata, A., 2016. A case study of $PM_{2.5}$ characterization in Bangi, selangor, Malaysia during the southwest monsoon season. Aerosol Air Qual. Res. 16 (11), 2685–2691.
Gao, Y., Arimoto, R., Duce, R., Zhang, X., Zhang, G., An, Z., Chen, L., Zhou, M., Gu, D., 1997. Temporal and spatial distributions of dust and its deposition to the China Sea. Tellus B 49, 172–189.
Gigliotti, C.L., Totten, L., Offenberg, J., Dachs, J., Reinfelder, J., Nelson, E., Gleeniv, T., Eisenreich, S., 2005. Atmospheric concentrations and deposition of polycyclic aromatic hydrocarbons to the Mid-Atlantic East Coast Region. Environ. Sci. Technol. 39, 5550–5559.
Guo, L., Chen, Y., Wang, F.J., Meng, X., Xu, Z.F., Zhuang, G.S., 2014. Effects of Asian dust on the atmospheric input of trace elements to the East China Sea. Mar. Chem. 163, 19–27.
Han, Y.M., Cao, J.J., Chow, J.C., Watson, J.G., Fung, K., Jin, Z.D., Liu, S.X., An, Z.S., 2007. Evaluation of the thermal/optical reflectance method for discrimination between soot-and char-EC. Chemosphere 69, 569–574.
Han, Y.M., Han, Z.W., Cao, J.J., Chow, J.C., Watson, J.G., An, Z.S., Liu, S.X., Zhang, R.J., 2008. Distribution and origin of carbonaceous aerosol over a rural high-mountain lake area, Northern China and its transport significance. Atmos. Environ. 42, 2405–2414.
Han, Y.M., Cao, J.J., Lee, S.C., Ho, K.F., An, Z.S., 2010. Different characteristics of char and soot in the atmosphere and their ratio as an indicator for source identification in Xi'an, China. Atmos. Chem. Phys. 10, 595–607. https://doi.org/10.5194/acp-10-595-2010, 2010.
Han, Y.M., Chen, W.A., Huang, R.J., Chow, J.C., Watson, J.G., Ni, H.Y., Liu, S.X., Fung, K.K., Shen, Z.X., Wei, C., 2016. Carbonaceous aerosols in megacity Xi'an, China: implications of thermal/optical protocols comparison. Atmos. Environ. 132, 58–68.
Highwood, E.J., Kinnersley, R.P., 2006. When smoke gets in our eyes: the multiple impacts of atmospheric black carbon on climate, air quality and health. Environ. Int. 32, 560–566.
Hou, B., Zhuang, G.S., Zhang, R., Liu, T.N., Guo, Z.G., Chen, Y., 2011. The implication of carbonaceous aerosol to the formation of haze: revealed from the characteristics and sources of OC/EC over a mega-city in China. J. Hazard Mater. 190, 529–536.
Hsu, S.C., Liu, S., Arimoto, R., Liu, T., Huang, Y., Tsai, F., Lin, F., Kao, S., 2009. Dust deposition to the East China Sea and its biogeochemical implications. J. Geophys. Res. 114, D15304. https://doi.org/10.1029/2008JD01122.
Hsu, S.C., Wong, G., Gong, G., Shiah, F., Huang, Y., Kao, S., Tsai, F., Lung, S., Lin, F., Lin, I., 2010. Sources, solubility, and dry deposition of aerosol trace elements over the East China Sea. Mar. Chem. 120, 116–127.
Jacobson, M.Z., 2004. Sedimentation, dry deposition, and air-sea exchange. Fund. Atmospheric Modeling 661–672.
Jurado, E., Dachs, J., Duarte, C., Simó, R., 2008. Atmospheric deposition of organic and black carbon to the global oceans. Atmos. Environ. 42, 7931–7939.
Jurado, E., Jaward, F., Lohmann, R., Jones, K.C., Simó, R., Dahs, J., 2004. Atmospheric dry deposition of persistent organic pollutants to the Atlantic and inferences for the global oceans. Environ. Sci. Technol. 38, 5505–5513.
Jurado, E., Jawrad, F., Lohmann, R., Jones, K.C., Simó, R., Dachs, J., 2005. Wet deposition of persistent organic pollutants to the global oceans. Environ. Sci. Technol. 39, 2426–2435.
Kim, K.H., Sekiguchi, K., Furuuchi, M., Sakamoto, K., 2011. Seasonal variation of carbonaceous and ionic components in ultrafine and fine particles in an urban area of Japan. Atmos. Environ. 45 (8), 1581–1590.
Kunwar, B., Kawmaura, K., 2014. One-year observations of carbonaceous and nitrogenous components and major ions in the aerosols from subtropical Okinawa Island, an outflow region of Asian dusts. Atmos. Chem. Phys. 14 (4), 1819–1836.
Lee, C.T., Ram, S.S., Nguyen, D.L., Chou, C.C.K., Chang, S.Y., Lin, N.H., Chang, S.C., Hsiao, T.C., Sheu, G.R., Ou-Yang, C.F., Chi, K.H., Wang, S.H., Wu, X.C., 2016. Aerosol chemical profile of near-source biomass burning smoke in sonla, vietnam during 7-SEAS campaigns in 2012 and 2013. Aerosol Air Qual. Res. 16 (11), 2603–2617.
Li, T.C., Y, C.S, Huang, H.,C., Lee, C.L., Wu, S.P., Tong, C., 2017. Clustered long-range transport routes and potential sources of $PM_{2.5}$ and their chemical characteristics around the Taiwan Strait, Atmos. Environ. Times 148, 152–166.
Lin, T., Hu, L.M., Guo, Z.G., Zhang, G., Yang, Z.S., 2013. Deposition fluxes and fate of polycyclic aromatic hydrocarbons in the Yangtze River estuarine-inner shelf in the East China Sea. Global Biogeochem. Cycles 27, 77–87.
Masiello, C.A., 2004. New directions in black carbon organic geochemistry. Mar. Chem. 92, 201–213.
Menon, S., Hansen, J., Nazarenko, L., Luo, Y., 2002. Climate effects of black carbon aerosols in China and India. Science 297, 2250–2253.
Nakamura, T., Matsumoto, K., Uematsu, M., 2005. Chemical characteristics of aerosols transported from Asia to the East China Sea: an evaluation of anthropogenic combined nitrogen deposition in autumn. Atmos. Environ. 39, 1749–1758.
Park, J.S., Wade, T.L., Sweet, S., 2001. Atmospheric deposition of organochlorine contaminants to Galveston Bay, Texas. Atmos. Environ. 35, 3315–3324.
Sahu, R.K., Pervez, S., Chow, J.C., Watson, J.G., Tiwari, S., Panicker, A.S., Chakrabarty, R.K., Pervez, Y.F., 2018. Temporal and spatial variations of PM2.5 organic and elemental carbon in central India. Environ. Geochem. Health 1–18.
Schmidt, M., Skjemstad, J., Czimczik, C., Glaser, B., Prentice, K., Gelinas, Y., Kuhlbusch, T., 2001. Comparative analysis of black carbon in soils. Global Biogeochem. Cycles 15, 163–167.
Wang, F.W., Lin, T., Li, Y.Y., Ji, T.Y., Ma, C.L., Guo, Z.G., 2014. Sources of polycyclic aromatic hydrocarbons in $PM_{2.5}$ over the East China Sea, a downwind domain of East Asian continental outflow. Atmos. Environ. 92, 484–492.
Wang, F.W., Guo, Z.G., Lin, T., Hu, L.M., Chen, Y.J., Zhu, Y.F., 2015a. Characterization of carbonaceous aerosols over the East China Sea: the impact of the East Asian continental outflow. Atmos. Environ. 110, 163–173.
Wang, F.W., Guo, Z.G., Lin, T., Rose, N.L., 2016. Seasonal variation of carbonaceous pollutants in $PM_{2.5}$ at an urban 'supersite' in Shanghai, China. Chemosphere 146, 238–244.
Wang, F.W., Lin, T., Li, Y.Y., Guo, Z.G., Rose, N.L., 2017. Comparison of $PM_{2.5}$ carbonaceous pollutants between an urban site in Shanghai and a background site in a coastal East China Sea island in summer: concentration, composition and sources. Environ. Sci. Processes & Impacts 19, 833–842.
Wang, X.C., Li, A.C., 2007. Preservation of black carbon in the shelf sediments of the East China Sea. Chin. Sci. Bull. 52, 3155–3161.
Wang, J.Z., Ho, S.S., Cao, J.J., Huang, R.J., Zhou, J.M., Zhao, Y.Z., Xu, H.M., Liu, S.X., Wang, G.H., Shen, Z.X., 2015b. Characteristics and major sources of carbonaceous aerosols in $PM_{2.5}$ from Sanya, China. Sci. Total Environ. 530–531, 110–119.
Zhang, X.Y., Arimoto, R., An, Z.S., 1997. Dust emission from Chinese desert sources linked to variations in atmospheric circulation. J. Geophys. Res. 102, 28041–28047.
Zhang, Y., Yu, Q., Ma, W.C., Chen, L.M., 2010. Atmospheric deposition of inorganic nitrogen to the eastern China seas and its implications to marine biogeochemistry. J. Geophys. Res. D00K10. https://doi.org/10.1029/2009JD012814.
Zhao, M., Qiao, T., Huang, Z., Zhu, M., Xu, W., Xiu, G.L., 2015. Comparison of ionic and carbonaceous compositions of $PM_{2.5}$ in 2009 and 2012 in Shanghai, China. Sci. Total Environ. 536, 695–703.
Zhu, C.S., Chen, C.C., Cao, J.J., Tsai, C.J., Chou, C.K., Liu, S.C., Roam, G.D., 2010. Characterization of carbon fractions for atmospheric fine particles and nanoparticles in a highway tunnel. Atmos. Environ. 44 (23), 2668–2673.
Zhu, C.S., Cao, J.J., Tsai, C.J., Shen, Z.X., Han, Y.M., Liu, S.X., Zhao, Z.Z., 2014. Comparison and implications of $PM_{2.5}$ carbon fractions in different environments. Sci. Total Environ. 203, 466–467.
Zhu, C.S., Cao, J.J., Tsai, C.J., Shen, Z.X., Liu, S.X., Huang, R.J., Zhang, N.N., Wang, P., 2016. The rural carbonaceous aerosols in coarse, fine, and ultrafine particles during haze pollution in northwestern China. Environ. Sci. Pollut. Res. 23 (5), 4569–4575.
Zhu, L., Chen, Y., Guo, L., Wang, F.J., 2013. Estimate of dry deposition fluxes of nutrients over the East China Sea: the implication of aerosol ammonium to non-sea-salt sulfate ratio to nutrient deposition of coastal oceans. Atmos. Environ. 69, 131–138.